Disposable Fluidic Actuators for Miniature In-Vivo Surgical Robotics

Abolfazl Pourghodrat
Department of Mechanical and Materials Engineering,
University of Nebraska-Lincoln,
W342 Nebraska Hall,
Lincoln, NE 68588-0526
e-mail: a.pourghodrat@gmail.com

Carl A. Nelson[1]
Mem. ASME
Department of Mechanical and Materials Engineering,
University of Nebraska-Lincoln,
W342 Nebraska Hall,
Lincoln, NE 68588-0526
e-mail: cnelson5@unl.edu

Fusion of robotics and minimally invasive surgery (MIS) has created new opportunities to develop diagnostic and therapeutic tools. Surgical robotics is advancing from externally actuated systems to miniature in-vivo robotics. However, with miniaturization of electric-motor-driven surgical robots, there comes a trade-off between the size of the robot and its capability. Slow actuation, low load capacity, sterilization difficulties, leaking electricity and transferring produced heat to tissues, and high cost are among the key limitations of the use of electric motors in in-vivo applications. Fluid power in the form of hydraulics or pneumatics has a long history in driving many industrial devices and could be exploited to circumvent these limitations. High power density and good compatibility with the in-vivo environment are the key advantages of fluid power over electric motors when it comes to in-vivo applications. However, fabrication of hydraulic/pneumatic actuators within the desired size and pressure range required for in-vivo surgical robotic applications poses new challenges. Sealing these types of miniature actuators at operating pressures requires obtaining very fine surface finishes which is difficult and costly. The research described here presents design, fabrication, and testing of a hydraulic/pneumatic double-acting cylinder, a limited-motion vane motor, and a balloon-actuated laparoscopic grasper. These actuators are small, seal-less, easy to fabricate, disposable, and inexpensive, thus ideal for single-use in-vivo applications. To demonstrate the ability of these actuators to drive robotic joints, they were modified and integrated in a robotic arm. The design and testing of this surgical robotic arm are presented to validate the concept of fluid-power actuators for in-vivo applications. [DOI: 10.1115/1.4035005]

Introduction

Bleeding, infection, and pain are major concerns in surgery, afflicting patients for decades. Minimizing the invasiveness of surgery through minimally invasive techniques is believed to improve patient outcomes by reducing these concerns. Surgical robotics is a recent trend in surgery intended to overcome some of the complexities introduced by minimally invasive surgery (MIS), such as difficult visualization, reduced dexterity, restricted workspace, and nonintuitive controls.

Surgical robotics is advancing from externally actuated systems such as the da Vinci® Surgical System [1] to miniature in-vivo robotics where the entire robot is inserted into the patient's body [2–14]. However, with miniaturization of surgical robots, there comes a trade-off between the size of the robot and its capability [15]. Miniature electric motors have been used in many in-vivo robots [2–14] as the primary means of actuation. Slow actuation, low load capacity, sterilization difficulty, leaking electricity and transferring produced heat to tissues, and high cost are among the key limitations of the use of electric motors in in-vivo applications [15–17].

The hypothesis of the research presented here was that the inherent high power density of fluids in the form of pneumatics or hydraulics can be leveraged to build surgical robotic systems that can meet the size, speed, and force requirements without compromising one design requirement for another. Fluid power has higher power density on the order of 2:1 or greater when compared with electric motors (see Table 1).

Hollerbach et al. [18] conducted a thorough study of different actuator technologies used in several robotic projects. They compared the characteristics of the following actuators: an electromagnetic motor, an electrohydraulic rotary actuator, an electropneumatic servo-valve, a NiTi shape memory alloy (SMA), a polyvinyl alcohol/polyacrylic acid polymer actuator, a piezoelectric motor, a magnetoelastic wave motor, and human biceps muscle. Their findings indicated that hydraulic actuators have the overall best characteristics (torque and power density) with design advantages for bandwidth, intrinsic compliance, and packaging. This study along with several other studies [19,20] suggests that fluidic (hydraulic and pneumatic) actuators deliver among the highest force and power densities at small length scales.

This means of actuation is compatible with the harsh in-vivo environment, removing the aforementioned concerns with using onboard electric motors. To actuate robotic joints hydraulically, two types of actuators are typically required: a linear actuator (a hydraulic cylinder) and a rotary actuator (a hydraulic motor). Commercially available miniature hydraulic cylinders and motors were not found suitable, mainly due to relatively large size and poor sealing under operating pressure on the order of 400 kPa (approximately 60 psi). Accordingly, novel seal-less fluidic linear and rotary actuators were built. These actuators are easy to fabricate, inexpensive, and can be customized to the sizes required for in-vivo applications. Design, prototyping, testing of the actuators, and a robotic arm built using them are described in this paper.

Related Work. Rentschler et al. [6] developed a series of miniature in-vivo robots assisting surgeons by providing visual feedback. A family of wheel-driven modular wireless robots capable of exploring the abdominal cavity and performing some

Table 1 Comparison of actuator characteristics [17]

Characteristics	Electric	Hydraulic	Pneumatic
Power-to-weight ratio (W/kg)	25–150	650	300
Force to cross-sectional area (N/cm^2)	0.3–1.5	2000	100

[1]Corresponding author.

Manuscript received January 4, 2016; final manuscript received September 27, 2016; published online December 21, 2016. Assoc. Editor: Venketesh Dubey.

surgical-assist tasks was also developed and tested in porcine models [7]. In attempts to perform more complicated surgical tasks, several versions of a two-arm miniature in-vivo robotic platform with varying degrees of freedom have been designed, built, and tested in porcine models [2–4] with promising results for single-incision laparoscopic surgery (SILS). The way these robots are operated mimics more closely the method in which laparoscopic procedures are carried out. Lehman et al. [5,17] built a tethered bimanual robot for natural orifice transluminal endoscopic surgery (NOTES), which is inserted through the mouth, enters the peritoneal cavity though the esophagus and an internal incision in the stomach, and attaches magnetically to the abdominal wall. In a similar work, Di Natali et al. [8] designed and built a magnetically actuated surgical platform for SILS.

Recent development has focused on design of snakelike robots for NOTES. Several generations of a multifunctional snake robot for NOTES have been built and tested [9,10]. A multiple-instrument manipulator is delivered to the surgical site using a snake robot. In related work, researchers have built robotic modules that are meant to be ingested and assembled into a reconfigurable articulated mechanism inside the stomach to perform screening and interventions in the gastrointestinal tract [11].

While most of the developed surgical robots are primarily actuated by electric motors, there are a few medical robotic systems driven by fluid power. The HeartLander robot, an inchwormlike robot delivering therapy to the surface of a beating heart, is a rare example of a nonmotor-driven surgical robot driven by suction force [13,14]. Berg [15] developed a novel, dexterous hydraulic robotic surgical tool for transgastric natural orifice surgery. In a related vein, researchers have created fluid-based locomotion mechanisms to propel colonoscopy tools inside the large intestine [21–23].

Methods

Fluidic Linear Actuator. Hydraulic cylinders are the main linear actuators used in many hydraulic robotics. A double-acting cylinder is required to cause flexion and extension of a revolute joint.

Most off-the-shelf double-acting cylinders with high-pressure ratings are quite bulky, mostly due to seals between the piston and cylinder and fittings used to connect the tubing to the cylinder. Those that are small in diameter and short in length are single-acting with poor sealing under high pressure, and thus, unable to output adequate force to meet surgical requirements. These commercially available cylinders come with a stroke that is usually either larger or smaller than is desirable for driving a robotic joint at this size scale. Thus, there is a need for fabrication of customized hydraulic cylinders. Fabrication of miniature but powerful hydraulic cylinders within the desired size range has been a challenge due to difficulties in sealing at operating pressure, obtaining necessary surface finishes, and associated cost of fabrication. This motivated us to build a miniature seal-less double-acting pneumatic/hydraulic cylinder.

Table 2 lists the design requirements specifications for the linear actuator. The outer diameter (OD) of the cylinder should be less than 11 mm so that the overall diameter of a bimanual robot (with the arms parallel) is less than a typical esophagus diameter, which is approximately 22 mm [9]. The length of the cylinder should be less than 25 mm so that it can fit in a typical miniature robotic arm [10]. The stroke of the cylinder needs to be on the range of 2–6 mm for typical joint and tool actuation. The cylinder should be capable of delivering a minimum force of 2.5 N [24,17] required to perform surgical tasks. The linear actuator should be a double-acting cylinder to provide a reciprocating motion needed to drive most robotic joints and/or some surgical tools.

Table 2 The linear actuator design requirements specifications

Req. ID	Description
LARS-01	OD of the linear actuator should be less than 11 mm
LARS-02	Stroke of the linear actuator should be between 2 and 6 mm
LARS-03	Length of the linear actuator should be less than 25 mm
LARS-04	The linear actuator should be capable of delivering a minimum force of 2.5 N
LARS-05	The linear actuator should be double-acting

Taking into account the design requirements, a novel miniature cylinder was created. It consists of an outer tube, an inner tube, a piston, a pin, and two off-the-shelf latex balloons, as depicted in Fig. 1. The novelty of this concept is in the use of elastomeric balloons in both upper and lower chambers of the inner tube to drive the piston. When the balloon is pressurized, it inflates and pushes the piston up/down. A metal pin and groove system is used to transfer force from the piston to the outer tube. The inner tube is stationary, and the outer tube can extend or contract depending upon the direction of the piston motion. The balloon itself is sealed onto a polyvinyl chloride (PVC) tube with an OD of 3.9 mm using either heat-shrink tube or a press fit between the hole on the inner tube and the PVC tube with the balloon. Custom parts were made using a 3D printer and/or laser cutting machine (Fig. 2). The bore, OD, length, and stroke of the cylinder are 5.9, 11, 22.8, and 6 mm, respectively. This indicates that all the size requirements (Req. ID: LARS-01–LARS-03) specified in Table 2 have been met. This linear actuator is small, seal-less, rod-less, leak-free, easy to fabricate, inexpensive, and disposable, thus ideal for single-use in-vivo applications.

Bench-top testing was performed to characterize the performance of the linear actuator (Fig. 3). Pressure was varied for a constant load, and the total displacement (stroke) of the first-generation actuator was measured; the results are plotted in Fig. 4.

The primary results indicated that the actuator is capable of providing approximately 7 N of force with 4 mm stroke at 0.38 MPa (55 psi). This indicates that the force requirement (Req. ID: LARS-04) has been satisfied.

The burst pressure of the balloon was measured to be 0.62 MPa (90 psi) for a 6 mm stroke. The cylinder underwent an average of 300 cycles under an average pressure of 0.38 MPa (55 psi) before the balloon yielded. The output force efficiency of this cylinder was calculated to be approximately 68% which is somewhat comparable with 80% efficiency found in high-quality, commercially available pneumatic cylinders.

Fluidic Rotary Actuator. There is no miniature hydraulic motor (in the range of 15×15 mm, small enough for in-vivo robots) commercially available nor in the prior art to the best of our knowledge. This motivated us to design and create a miniature rotary actuator, which is small, potent, and easy to fabricate.

Table 3 summarizes the design requirements specifications for the rotary actuator. The rotary actuator should be 15×15 mm, the same size as the DC motor [26], which has been used in many previous in-vivo robots for SILS [2–4]. Revolute joints in previous SILS robot designs do not require continuous rotation; the rotary actuator should have a 180 deg range of motion. The motor velocity should be greater than 0.486 rad/s [17]. High output torque is always a key factor in selection of small motors for in-vivo

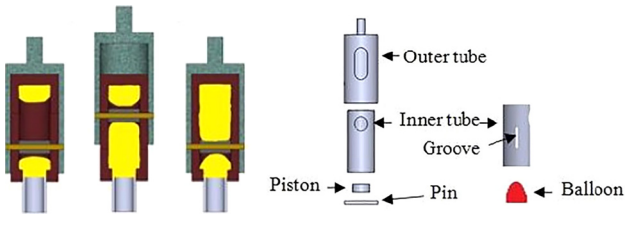

Fig. 1 Working principle of the linear actuator (left) and exploded view (right) [25]

Fig. 2 Linear actuator prototype [25]

Table 3 The rotary actuator design requirements specifications

Req. ID	Description
RARS-01	Size of the rotary actuator should be at most 15 × 15 mm
RARS-02	Motion range of the rotary actuator should be 180 deg
RARS-03	The rotary actuator speed should be greater than 0.486 rad/s
RARS-04	The rotary actuator should be capable of outputting a torque of 12 mNm

surgical robotics. Vane motors, compared with other types of hydraulic motors, are capable of outputting higher torque levels due to offering higher surface area against which hydraulic pressure can be applied. The rotary actuator should be a single-blade vane motor with output torque on the order of 12 mNm, which is

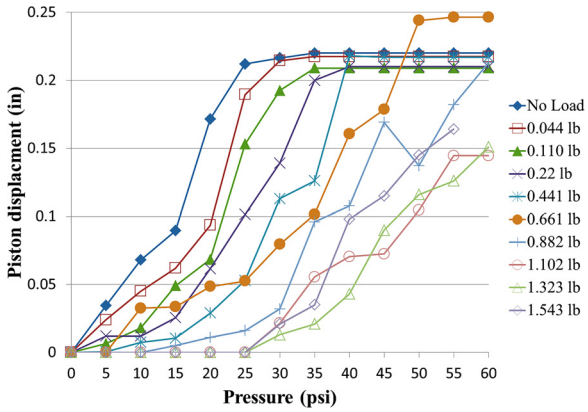

Fig. 4 Displacement versus pressure [25]

the maximum torque a similar 15 × 15 mm motor with a 112:1 gearhead can output (considering 59% efficiency) [26].

To meet the design requirements specifications (Table 3), a limited-motion vane motor with rotational range of motion of 180 deg was designed and built. The working principle is illustrated in Fig. 5. When the balloon is pressurized, it inflates and pushes the blade, causing it to rotate.

Three prototypes were fabricated, shrinking down the overall size of the motor from 25 × 25 mm to 18 × 18 mm to 15 × 15 mm in subsequent steps; this verifies that Req. ID: RARS-01 has been met. Most of the components were laser cut in acrylic with two miniature PVC tubes (OD = 2 mm) attaching to the motor. Regular off-the-shelf latex balloons or a medical grade balloon (latex balloon with an inner diameter of 13 French) from TechDevice Corporation, Watertown, MA, were used for prototyping the various prototypes. An exploded view of the motor is shown in Fig. 6.

To characterize the performance of the fluidic vane motor and compare it with a commercially available 15 × 15 mm electric DC motor, bench-top testing was performed (Fig. 7). A new motor with a medical grade balloon and a flange to attach to a fixture were built using a 3D printer and laser cutting machine. A flow meter, a flow control valve, a pressure regulator, and a pressure gauge were used to measure and adjust flow and pressure.

Figures 8 and 9 show the experimental characteristics of the vane motor. The flow rate was kept constant (4.25 L/min) for all the experiments; however, higher flow rate could result in higher speed and different speed–torque characterization. A minimum pressure of 69 kPa (10 psi) was required for the balloon to start expanding and making the rotor spin. The large difference between the experimental torque and the calculated torque could be due to errors in prototyping (misalignment, tolerances, etc.),

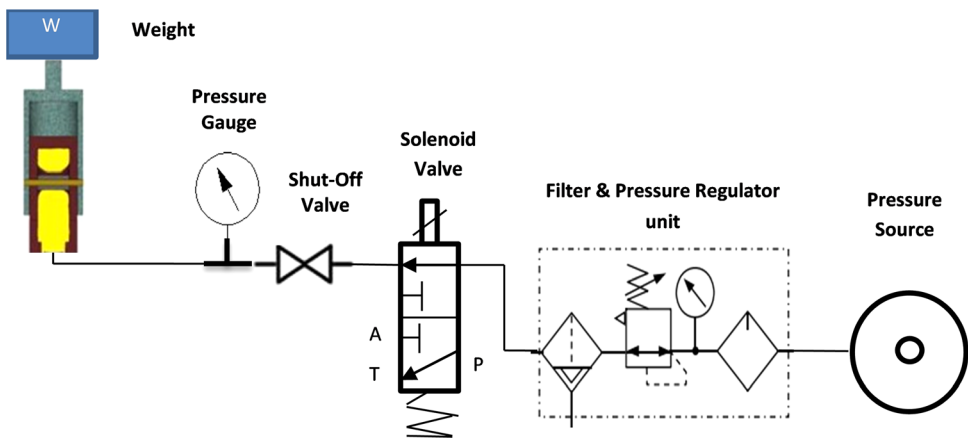

Fig. 3 Benchtop test setup

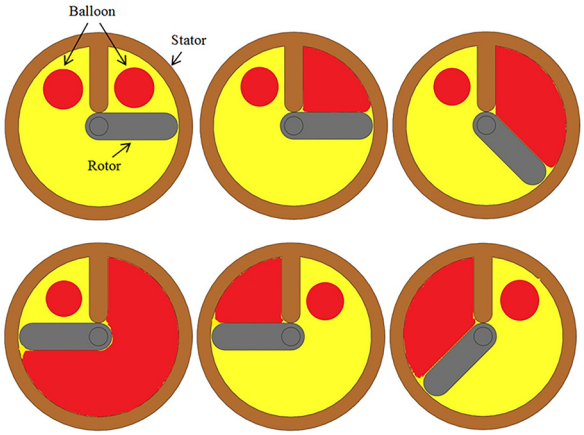

Fig. 5 Working principle of the vane motor

incomplete contacts between the balloon and the blade, and more importantly, the friction between the balloon and the stator wall and the top and bottom surfaces. A custom-made balloon with desired properties (higher elongation rate, higher burst pressure rate, and smaller wall thickness) could potentially improve the performance of the motor. Comparison between this fluidic vane motor and a Faulhaber 17 × 17 mm DC motor is summarized in Table 4.

The Faulhaber 17 × 17 mm DC motor has higher torque rating than the 15 × 15 mm version. The larger motor is used here to account for size differences between the 15 × 15 mm motor and the motor used for testing. A maximum torque of 18.5 mNm was achieved at 351.6 kPa (51 psi), providing almost eight times as much torque as a Faulhaber 17 × 17 mm DC motor delivers for

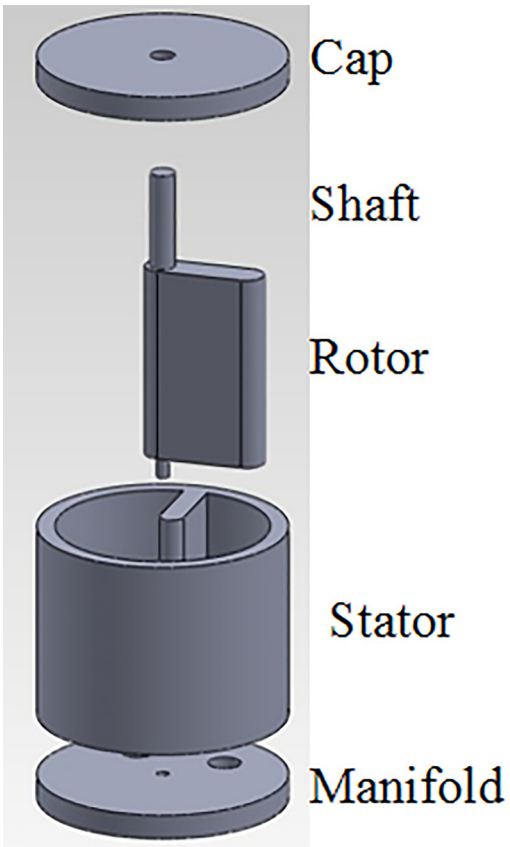

Fig. 6 Exploded view of the motor [25]

continuous rotation [26]. This indicates that the torque requirement (Req. ID: RARS-02) has been satisfied. The vane motor weighs 6 g (with no fluid) and 6.9 g if filed with water, approximately three times as light as the DC motor. The speed of the DC motor is much higher than the vane motor tested with a flow rate of 4.25 L/min. However, higher velocity could be achieved with higher flow rate. Nevertheless, the vane motor spins 180 deg in 1 s (3.14 rad/s) which is greater than the required 0.486 rad/s (Req. ID: RARS-03, Table 3).

Balloon-Actuated Grasper. The bulkiest part of the previous SILS robots [2–4] is the forearm where two electric DC motors with high reduction ratio gearheads and a rotary to linear motion converting mechanism are used for opening/closing and rotating the surgical grasper. In an effort to use fewer actuators and thereby decrease the size of the robot forearm, a normally closed grasper with a built-in actuator (a balloon) was developed with the design requirements specifications listed in Table 5. The size requirement is derived from the size of a typical 5 mm atraumatic grasper [27]. It has been reported that a pinch force on the order of 2.5–5 N is required for tissue manipulation in abdominal surgery [17].

After prototyping several iterations, a small and robust normally closed grasper was fabricated out of a laminar composite of metal and acrylic (Fig. 10). The grasper consists of a preloaded torsion spring that provides grasping force, an elastomeric balloon, two jaws, and a hinge pin. Pressurized air or water can be used to expand the balloon inside the grasper and open the jaws. The torsion spring was wound on a minilathe using 304 stainless steel spring wire with a diameter of 0.8 mm. The grasper size was measured to be 5 mm (W) × 16 mm (H) × 37 mm (L); this verifies that the size requirement has been satisfied.

Bench-top testing of the balloon-actuated grasper was performed. The testing results indicated a maximum grasping force of 3 N with tip displacement of 5.5 mm and a maximum tip displacement of 7 mm with grasping force of 2.3 N, using two springs with different stiffnesses achieved by varying the number of coils. The achieved pinch force and tip displacement meet the specified requirements (Table 5). A pressure of approximately 600 kPa (87 psi) was used to open the grasper. The opening/closure time was measured to be less than 1 s; this meets the speed requirement and is faster than the motor-driven graspers used in the previous robots [9,17].

This new method of tool actuation offers several advantages over electric-motor actuation. Manual operation of the grasper via a master user interface (similar to the system described in Ref. [28]) could be done in procedures where force feedback is desired. This would allow the surgeon to use his/her own fingers to actuate the instruments remotely, removing the need for an onboard haptic system that otherwise would require a larger amount of space inside the robot forearm. The grasper has a peak grasping force that can be set by either using torsional springs with different stiffnesses or controlling the pressure of the fluid inside the balloon ex vivo. This would contribute greatly to the safety of the patient with respect to the loss of tactile feedback during surgery, where excessive forces may be applied to tissues by the laparoscopic grasper during palpation, which could lead to tissue perforations and other similar trauma. While surgeons complain about the low actuation speed of the grasper in current SILS robots [17], the speed of the balloon-actuated grasper would exceed surgeons' expectations, enabling them to respond to tactile feedback and/or surgical traumas at human reaction speeds. With external actuation of the grasper, it becomes feasible to shrink the bulkiest part of the previous SILS robots (the forearm) almost 60% in diameter or in length.

Modeling of Balloon-Based Actuation. Figure 11 shows a free-body diagram of a simple balloon-based actuation. F_l is the load applied on the actuator, F_f is the friction force exerted on the

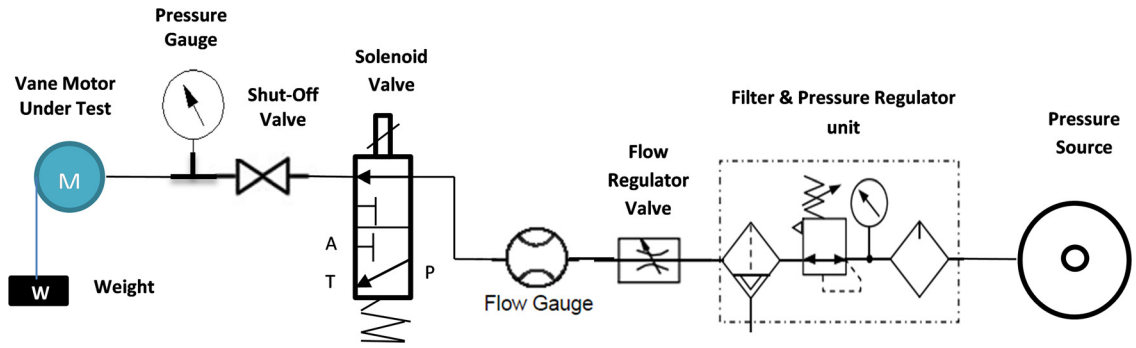

Fig. 7 Experimental testing setup

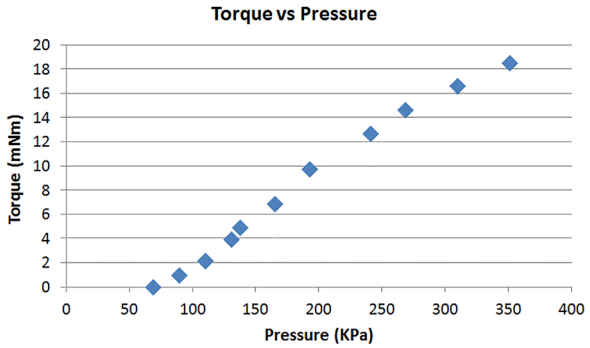

Fig. 8 Torque versus pressure for a constant flow rate of 4.25 L/min

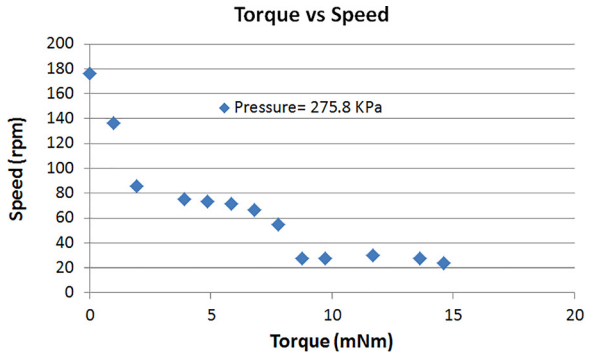

Fig. 9 Speed–torque characterization

expanding balloon from the container of the balloon, F_p is the force applied to the actuator from the fluid (air or water), and F_b is the elastic force caused by the elongation of the balloon. These forces can be found from the following equations:

$$F_l = F_p - F_f - F_b \tag{1}$$

$$F_p = pA \tag{2}$$

$$F_f = \mu F_c \tag{3}$$

Table 4 Comparison between a DC motor and the fluidic motor

Actuator	Max torque (mNm)	Weight (g)	No-load speed (rpm)
Fluid vane motor	18.5	6	180
Faulhaber 17 × 17 mm DC motor	2.2	18	14,000

where p is the fluid pressure delivered into the balloon, A is the cross-sectional area of the surface against which the balloon pushes, μ is the friction coefficient, and F_c is the circumferential force applied to the balloon container that can be easily calculated by multiplying the pressure by the circumferential area of the balloon in contact with the container. μ is a function of the surface finish of the internal wall of the balloon container and the balloon material. μ could be determined empirically for different actuators.

To determine F_b, a model detailed in Ref. [29] can be used. This model derives a relationship between the force applied to an elastomer and its extension.

A similar approach could be used to measure the Young's modulus of the balloon used in the fluidic linear actuator. Young's modulus can be used then to calculate F_b as follows:

$$F_b = \frac{EA_0\Delta L}{L} \tag{4}$$

where E is the Young's modulus, A_0 is the original cross-sectional area, ΔL is the balloon extension, and L is the original length of the balloon.

Additionally, a similar method to that described in Ref. [30] can be used to take into account the Mullins effect and cyclic stress softening of filled elastomers. The Mullins effect states that in filled rubbers, the stress–strain graph depends on the maximum loading the rubber has experienced previously.

In a simplified model, Eqs. (1)–(4) are used to calculate the output force of the balloon-based linear actuator described at the beginning of the "Methods" section. The Young's modulus is assumed to be 0.0453 MPa according to Ref. [29] for a similar material to TC-5005 silicone. A_0, L, and ΔL of the balloon were assumed to be 4.7 mm^2, 3 mm, and 4 mm, respectively, based on typical characteristics of the actuators under consideration. Substituting these values in Eq. (4), F_b is calculated to be 0.284 N. Assuming a pressure of 0.38 MPa which is the pressure used for testing of the linear actuator, F_c and F_p are calculated to be 21.12 N and 10.38 N, respectively. μ is assumed to be 0.05, which is a friction coefficient based on a well-lubricated interface, thus providing an optimistic estimate. F_f is calculated to be 1.06 N using Eq. (3). Substituting the values calculated for F_f, F_p, and F_b into Eq. (1), F_l is calculated to be 9.04 N.

Table 5 The grasper design requirements specifications

Req. ID	Description
GRS-01	The grasper size should be at most 5 mm (W) × 22 mm (H) × 49 mm (L)
GRS-02	The grasper pinch force should be on the order of 2.5–5 N
GRS-03	The grasper should have a minimum tip displacement of 5 mm
GRS-04	It should take less than 2 s for the grasper to open or close

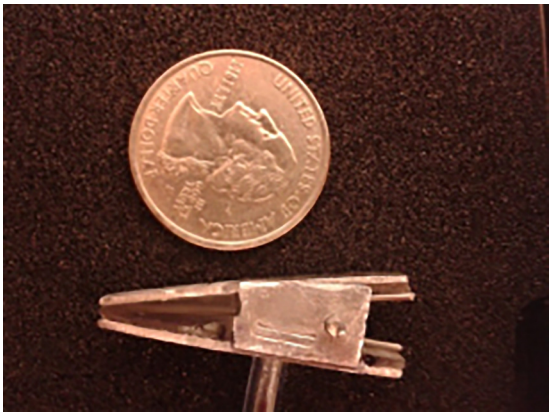

Fig. 10 Laparoscopic grasper prototype [25]

The output force achieved from the benchtop testing, 7 N, is close to the 9 N predicted by this model. A more accurate model could be achieved knowing the mechanical properties of the balloon. The elastic force, F_b, which counteracts the output force of the actuator, seems to be negligible compared to the force, 10.38 N, applied to the piston by the fluid pressure. However, the friction force is relatively large and should be minimized to improve the efficiency of the actuator.

Fluid-Powered Robot Arm. The vision of this work is to develop a fully hydraulically driven miniature bimanual robot for natural orifice translumenal endoscopic surgery (NOTES). However, it was deemed wise to first build one arm using the linear actuator, the vane motor, and a tool-changing manipulator described in Ref. [28]. The robot arm, seen in Fig. 12, has three degrees of freedom in addition to one degree of freedom of opening and closing the instruments. The first prototype was built to demonstrate the proof of concept and investigate the functionality of the fluidic actuators.

One of the main advantages of the developed actuators is the ease of fabrication and the flexibility of integrating them in different designs. These actuators were redesigned and fabricated according to intended application, size limitation, and connection method. The actuators can be driven either hydraulically or pneumatically. They were tested with both fluids (water and air) separately with successful results before their integration into the system. When tested with water, bleeding the air out of these balloon-based actuators was difficult since one end of the balloon is closed. A syringe with a long, thin needle was used to inject water in the balloon and push the air out. For initial testing of the robot arm, it was decided to use pneumatics due to ease of setup, availability of pneumatic components, and not having to deal with filling the entire system with water and bleeding the air out of the system. Future work includes developing a master control system similar to the system described in Ref. [28] to allow use of water instead of air and obtain a precise and inexpensive position control for the linear actuator and the vane motor. Moreover, replacing pressurized air with water reduces the safety risks associated with balloon failure, since water is considered incompressible and would not expand in the abdominal cavity in the event of pressure release.

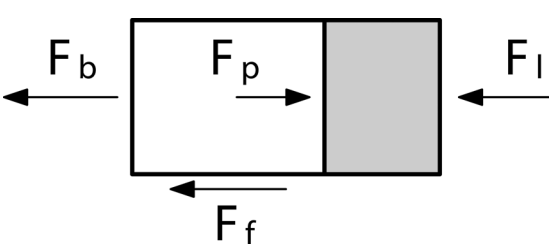

Fig. 11 Free-body diagram of a balloon-based actuation

Design. Figure 13 shows the detailed design of the vane motor used to rotate the base of the robot arm, providing the roll degree of freedom (DOF). This motor is a customized version of the limited-motion rotary actuator presented above. Two miniature high-precision stainless steel ball bearings (McMaster-Carr, 57155K341 and 7804K111) were mounted in the flange and the cap to facilitate rotation of the motor shaft and support radial and axial load. A connecting link (connector in Fig. 13) was added to the motor, allowing easy attachment of other parts to the motor and providing room for routing plastic tubing transferring fluid. The cap was glued to the stator using cyanoacrylate glue.

To give the manipulator a yaw-type rotational DOF, a linear actuator with a linear to rotary converter was used. The linear actuator is another customized version of the linear actuator described above with a stroke of 6 mm. A plastic rack–pinion gear set with a module of 0.5 mm was used to convert the cylinder's linear motion to the joint's rotary motion. The rack gear (Gizmoszone, GRG0.5-125) was glued to the top of the outer tube of the cylinder. The pinion gear (Gizmoszone, GM0.5-08-19) was glued to the link connecting the manipulator to the joint. Two small ball bearings (McMaster-Carr, 57155K339) were used to provide rolling support for the rack gear and to facilitate translating movement of the rack gear.

Most parts of the robot arm were fabricated out of acrylonitrile-butadiene-styrene material using a 3D printer. Regular off-the-shelf latex balloons were used in the linear and rotary actuators. The actuators, multi-instrument manipulator, and all the other subcomponents were assembled together to make a fluid-powered robot arm (Fig. 14).

Testing Results. To test the functionality of the robot arm, bench-top testing was performed. A simple control setup consisting of a compressor, a pressure regulator, a flow meter, a flow control valve, and two directional control solenoid valves was used to run the linear actuator and the vane motor. Testing of the multifunctional manipulator is presented in Ref. [28].

Each actuator was run separately. The vane motor was able to rotate the entire robot arm 180 deg in both directions (clockwise and counterclockwise) in 0.61 s with a flow rate of 5.2 L/min and a pressure of approximately 0.345 MPa (50 psi). The linear actuator with rack and pinion gear set was able to rotate the elbow joint

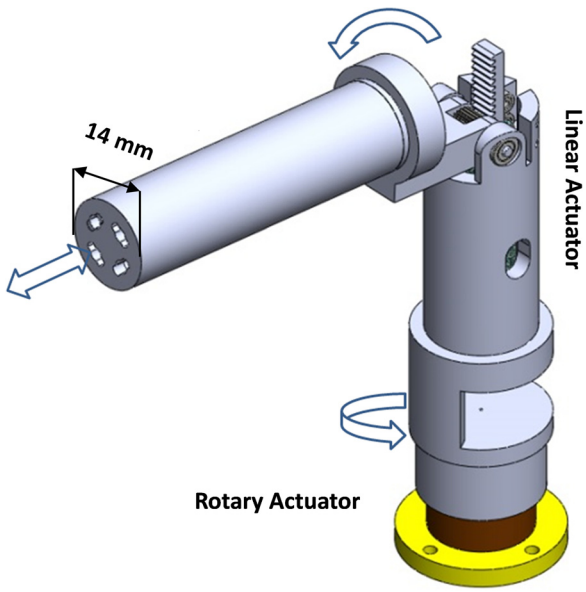

Fig. 12 Robotic arm 3D model

nearly 100 deg clockwise (upward) and counterclockwise (downward) in 19 and 3 s, respectively, with the same flow rate and pressure as used for the vane motor. While gravity helped the manipulator to move downward faster, there were other factors that could cause the speed difference between clockwise and counterclockwise displacement of the elbow joint. These factors include: a poor mate between the rack gear and the pinion gear, radial expansion of the balloon in the upper chamber of the linear actuator compared to axial expansion in the lower chamber, and friction in the moving parts. A better surface finish on the back of the rack gear where it has a continual contact with two small ball bearings providing rolling support could decrease the friction and lead to a better mate between the rack gear and the pinion gear. A customized *L*-shaped balloon could be used in the upper chamber of the linear actuator so that the balloon will expand axially. The entire robot arm with four instruments weighs approximately 50 g.

Conclusions

The field of surgery is moving toward less invasive techniques to improve patient outcomes. The dream of scar-free surgery is becoming a reality with advancements in surgical tools and imaging technology. Fusion of robotics and surgery has created a unique opportunity to develop novel devices for implementation of minimally invasive techniques. The new trend in surgical robotics is development of miniature in-vivo robots that can enter the human body from natural orifices for diagnosis and treatment. It is believed that SILS and NOTES are important parts of the future of surgery with their great potential benefits resulting from minimizing external incisions. The primary choice of actuation in many of the previous surgical robotic devices has been electric motors. While some of these miniature in-vivo systems have demonstrated promising results, many of them encountered the challenge of balance between scale and robotic capability. Moreover, the nature of inserting electric motors inside the body among biological tissues and organs introduces additional design concerns and limitations such as the risk of leaking electricity to tissues, transferring heat from motors to the organs, and difficulty in sterilizing electronics. With the current state of technology in building electric motors, it appears very difficult to solve the scale-power challenge and move past the in-vivo introduced concerns/limitations.

Fluid power in the form of hydraulics or pneumatics has a long history in driving many industrial devices. Many simple fluidic medical devices are either commercially available or have been reported in the literature. The hypothesis for this research was that fluid power could be exploited in development of miniature in-vivo surgical robots. High power density and good compatibility with the in-vivo environment are the key advantages of fluid power over electric motors when it comes to in-vivo applications.

To build a fluid-powered robot, it was first necessary to develop small fluidic actuators to drive robot joints and impart force and torque to surgical tools. A miniature cylinder and a limited-motion vane motor were built. These balloon-based actuators are small, powerful, easy to fabricate, and inexpensive, ideal for disposable applications. Testing of these actuators showed promising results. The performance of these actuators could be enhanced by the use of customized balloons with improved properties. Fabrication of a customized balloon was beyond the scope of this research and is left for future work. Simulation of the balloon-based actuation was difficult due to unknown properties of the balloons and the latex tubes used in this research. However, balloons could be custom-made and mechanical characterization testing could be performed, potentially leading to a model for simulating these actuators. Air, water, or saline could be used in these actuators. While air is clean and available in many operating rooms, control difficulty, cost of control hardware, and risk of leaking into the body are limitations for use in in-vivo surgical robotics. Water and saline are better choices, although bleeding the air out of the system can be difficult.

The fluidic actuators and an electrohydraulic manipulator were used to build a surgical robot arm. Bench-top testing of the robot arm confirmed the usability of the newly developed actuators in in-vivo surgical robotics; however, further characterization and testing of the robot arm are part of future work. The vision of this research is to make a bimanual robot for NOTES using two of these arms connected together and delivered to the abdominal

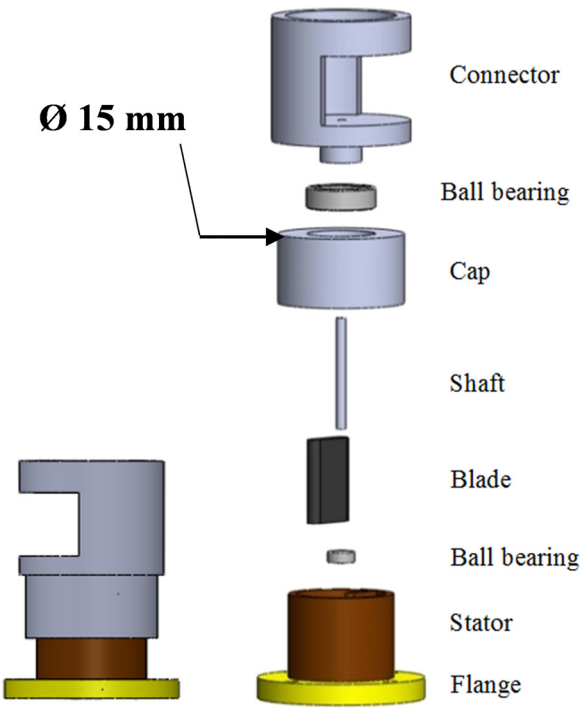

Fig. 13 Vane motor 3D model and exploded view

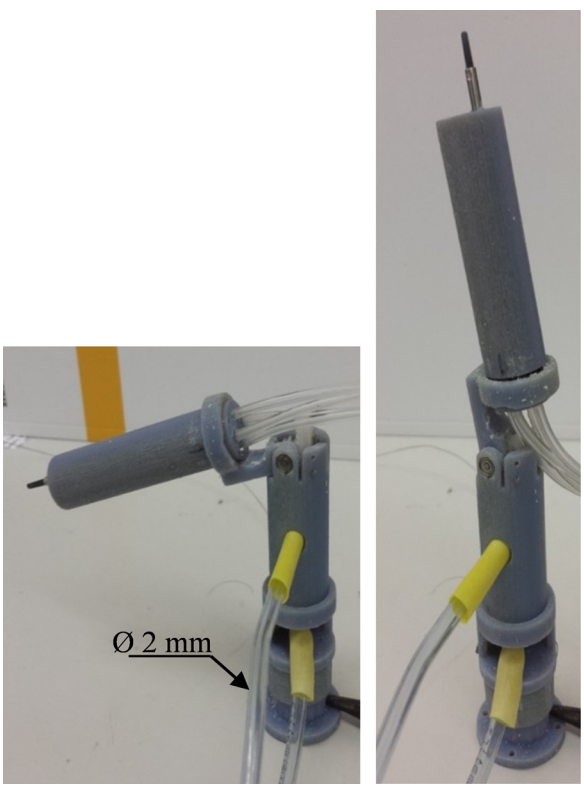

Fig. 14 Fluid-powered robotic arm prototype

cavity by a snake robot as described in Refs. [9] and [10]. The work described in Ref. [10] details an insertion/retraction mechanism that enables deployment of a bimanual robot with the arms' outer diameter less than 22 mm (a typical esophagus diameter is approximately 22 mm [9]). This would be the first fully hydraulically driven bimanual robot for NOTES with up to eight surgical instruments available at the site of surgery.

Acknowledgment

The authors gratefully acknowledge the support from NIH under Grant No. 1 R21 EB015017-01A1.

References

[1] Intuitive Surgical, 2014, "The da Vinci Surgical System," Intuitive Surgical, Inc., Sunnyvale, CA, accessed June 3, 2014, www.intuitivesurgical.com/products/davinci_surgical_system/

[2] Wortman, T. D., Strabala, K. W., Lehman, A. C., Farritor, S. M., and Oleynikov, D., 2011, "Laparoendoscopic Single-Site Surgery Using a Multi-Functional Miniature In Vivo Robot," Int. J. Med. Robot. Comput. Assisted Surg., **7**(1), pp. 17–21.

[3] Wortman, T. D., Meyer, A., Dolghi, O., Lehman, A. C., McCormick, R. L., Farritor, S. M., and Oleynikov, D., 2012, "Miniature Surgical Robot for Laparoendoscopic Single-Incision Colectomy," Surg. Endoscopy, **26**(3), pp. 727–731.

[4] McCormick, R., Wortman, T., Strabala, K. W., Frederick, T. P., Oleynikov, D., and Farritor, S. M., 2011, "Kinematic and Workspace Comparison of Four and Five Degree of Freedom Miniature In Vivo Surgical Robot," ASME J. Med. Devices, **5**(2), p. 027533.

[5] Lehman, A. C., Dumpert, J., Wood, N. A., Redden, L., Visty, A. Q., Farritor, S., Varnell, B., and Oleynikov, D., 2009, "Natural Orifice Cholecystectomy Using a Miniature Robot," Surg. Endoscopy., **23**(2), pp. 260–266.

[6] Rentschler, M., Dumpert, J., Platt, S. R., Iagnemma, K., Oleynikov, D., and Farritor, S. M., 2007, "An In Vivo Mobile Robot for Surgical Vision and Task Assistance," ASME J. Med. Devices, **1**(1), pp. 23–29.

[7] Hawks, J., 2010, "Improved Mobile Wireless In Vivo Surgical Robots: Modular Design, Experimental Results, and Analysis," Ph.D. thesis, University of Nebraska-Lincoln, Lincoln, NE.

[8] Di Natali, C., Ranzani, T., Simi, M., Menciassi, A., and Valdastri, P., 2012, "Trans-Abdominal Active Magnetic Linkage for Robotic Surgery: Concept Definition and Model Assessment," IEEE International Conference on Robotics and Automation (ICRA), Saint Paul, MN, May 14–18, pp. 695–700.

[9] Seow, C. M., Chin, W. J., Nelson, C. A., Nakamura, A., Farritor, S. M., and Oleynikov, D., 2013, "Articulated Manipulator With Multiple Instruments for Natural Orifice Transluminal Endoscopic Surgery," ASME J. Med. Devices, **7**(4), p. 041004.

[10] Shen, T., Nelson, C. A., Warburton, K., and Oleynikov, D., 2015, "Design and Analysis of a Novel Articulated Drive Mechanism for Multifunctional NOTES Robot," ASME J. Mech. Rob., **7**(1), p. 011004.

[11] Harada, K., Oetomo, D., Susiloa, E., Menciassi, A., Daney, D., Merlet, J. P., and Dario, P., 2010, "A Reconfigurable Modular Robotic Endoluminal Surgical System: Visions and Preliminary Results," Robotica, **28**(2), pp. 171–183.

[12] Nagy, Z., Oung, R., Abbott, J. J., and Nelson, B. J., 2008, "Experimental Investigation of Magnetic Self-Assembly for Swallowable Modular Robots," IEEE/RSJ International Conference on Intelligent Robots and Systems, Nice, France, Sept. 22–26, pp. 1915–1920.

[13] Patronik, N., Zenati, M. A., and Riviere, C. N., 2004, "Crawling on the Heart: A Mobile Robotic Device for Minimally Invasive Cardiac Interventions," 7th International Conference on Medical Image Computing and Computer-Assisted Intervention, Saint-Malo, France, Sept. 26–29, Vol. 3217, pp. 9–16.

[14] Patronik, N., Zenati, M. A., and Riviere, C. N., 2005, "Preliminary Evaluation of a Mobile Robotic Device for Navigation and Intervention on the Beating Heart," Comput. Aided Surg., **10**(4), pp. 225–232.

[15] Berg, D. R., 2013, "Design of a Hydraulic Dexterous Manipulator for Minimally Invasive Surgery," Ph.D. dissertation, University of Minnesota Twin Cities, Minneapolis, MN.

[16] Berg, D. R., Li, P. Y., and Erdman, A. G., 2012, "Achieving Dexterous Manipulation for Minimally Invasive Surgical Robots Through the Use of Hydraulics," ASME Paper No. DSCC2012-MOVIC2012-8685.

[17] Lehman, A. C., 2012, "Miniature In Vivo Robots for Minimally Invasive Surgery," Ph.D. thesis, University of Nebraska-Lincoln, Lincoln, NE.

[18] Hollerbach, J. M., Hunter, I. W., and Ballantyne, J., 1992, "A Comparative Analysis of Actuator Technologies for Robotics," *The Robotics Review*, Vol. 2, MIT Press Cambridge, MA, pp. 299–342.

[19] Granosik, G., and Borenstein, J., 2006, "Pneumatic Actuators for Serpentine Robot," *Climbing and Walking Robots*, Springer, Berlin, pp. 719–726.

[20] De Volder, M., and Reynaerts, D., 2010, "Pneumatic and Hydraulic Microactuators: A Review," J. Micromech. Microeng., **20**(4), p. 043001.

[21] Pourghodrat, A., Dehghani, H., Nelson, C. A., Oleynikov, D., Dasgupta, P., and Terry, B. S., 2014, "Disposable Fluidic Self-Propelling Robot for Colonoscopy," ASME J. Med. Devices, **8**(3), p. 039301.

[22] Kim, B., Lim, H. Y., Park, J. H., and Park, J. O., 2006, "Inchworm-Like Colonoscopic Robot With Hollow Body and Steering Device," JSME Int. J. Ser. C, **49**(1), pp. 205–212.

[23] Shike, M., Fireman, Z., Eliakim, R., Segol, O., Sloyer, A., Cohen, L. B., Goldfarb-Albak, S., and Repici, A., 2008, "Sightline ColonoSight System for a Disposable, Power-Assisted, Non-Fiber-Optic Colonoscopy (With Video)," Gastrointest. Endoscopy, **68**(4), pp. 701–711.

[24] De Visser, H., Heijnsdijk, E. A., Herder, J. L., and Pistecky, P. V., 2002, "Forces and Displacements in Colon Surgery," Surg. Endoscopy, **16**(10), pp. 1426–1430.

[25] Pourghodrat, A., and Nelson, C. A., 2013, "Miniature Fluidic Actuators for Surgical Robotics," ASME J. Med. Devices, **8**(3), p. 030920.

[26] Faulhaber, 2015, "DC-Micromotors," FAULHABER Miniature Drive Systems, Switzerland, accessed Dec. 3, 2015, http://www.faulhaber.com/

[27] Symmetry Surgical, 2015, "Laparoscopic Portfolio," Symmetry Surgical, Symmetry Surgical, Inc., Antioch, TN, accessed Aug. 2, 2015, http://www.symmetrysurgical.com

[28] Pourghodrat, A., Nelson, C., and Oleynikov, D., 2014, "Electrohydraulic Robotic Manipulator With Multiple Instruments for Minimally Invasive Surgery," ASME J. Med. Devices, **8**(3), p. 030919.

[29] Soleimani, M., 2003, "Development of a Novel Balloon-Shape Electroactive Polymer (EAP) Actuator," Master's thesis, Simon Fraser University, Burnaby BC, Canada.

[30] Cantournet, C., Desmorat, R., and Bessona, J., 2009, "Mullins Effect and Cyclic Stress Softening of Filled Elastomers by Internal Sliding and Friction Thermodynamics Model," Int. J. Solids Struct., **46**(11–12), pp. 2255–2264.